Local Minimization of Motor Torques on Robots with Elastic Joints

Federico Baldisseri, Arturo Maiani

September 26, 2021

Contents

1 Introduction

In robotics, the rigidity assumption on the couplings between motors and joints is not always precisely descriptive. This paper will focus on exploiting redundancy in a 3R planar robot with elastic joints in order to locally minimize the weighted norm of the motor torque vector.
First of all, a dynamic model for the 3R planar robot with elastic joints is built. Then, a local optimization is performed with different weighting matrices for the norm of the torque vector. Thus, this study is enforced with several simulations performing linear and circular paths. An analysis of the corresponding performances will be presented, in order to determine the best approach for each case.

2 Robot Dynamic model

The direct kinematics for the planar 3R robot are given by:

$$\begin{pmatrix} p_x \\ p_y \end{pmatrix} = \begin{pmatrix} l_1 c_1 + l_2 c_{12} + l_3 c_{123} \\ l_1 s_1 + l_2 s_{12} + l_3 s_{123} \end{pmatrix}$$

The velocities of the centers of mass are given by:

$$v_{c1} = \begin{pmatrix} -d_1 s_1 \dot{q_1} \\ d_1 c_1 \dot{q_1} \end{pmatrix} \qquad v_{c2} = \begin{pmatrix} -d_1 s_{12}(\dot{q_1} + \dot{q_2}) - l_1 s_1 \dot{q_1} \\ d_1 c_{12}(\dot{q_1} + \dot{q_2}) + l_1 c_1 \dot{q_1} \end{pmatrix}$$

$$v_{c3} = \begin{pmatrix} -l_2 s_{12}(\dot{q_1} + \dot{q_2}) - d_3 s_{123}(\dot{q_1} + \dot{q_2} + \dot{q_3}) - l_1 s_1 \dot{q_1} \\ l_2 c_{12}(\dot{q_1} + \dot{q_2}) + d_3 c_{123}(\dot{q_1} + \dot{q_2} + \dot{q_3}) + l_1 c_1 \dot{q_1} \end{pmatrix}$$

In order to obtain the robot dynamic model, we shall first derive the Lagrangian function of the system. Since the robot lies on a horizontal plane, the potential energy is only elastic.
We will get model of the general form:

$$M(z)\ddot{z} + c(z, \dot{z}) + \left(\frac{\partial U}{\partial z}\right)^T = \tau_z \qquad where\ z = \begin{pmatrix} q \\ \theta \end{pmatrix},\ \tau_z = \begin{pmatrix} 0 \\ \tau \end{pmatrix}$$

We will derive the inertia matrix starting from the total kinetic energy of the system.

$$T_{l1} = \frac{1}{2} m_1 v_{c1}^T v_{c1} + \frac{1}{2} I_1 \dot{q_1}^2 \qquad T_{m1} = \frac{1}{2} I_{m1} \dot{\theta_1}^2 k_r^2$$

$$T_{l2} = \frac{1}{2} m_2 v_{c2}^T v_{c2} + \frac{1}{2} I_2 (\dot{q_1} + \dot{q_2})^2 \qquad T_{m2} = \frac{1}{2} I_{m2} \dot{\theta_2}^2 k_r^2 + \frac{1}{2} m_{m2} v_1^T v_1$$

$$T_{l3} = \frac{1}{2}m_3 v_{c3}^T v_{c3} + \frac{1}{2}I_2(\dot{q}_1 + \dot{q}_2 + \dot{q}_3)^2 \qquad T_{m3} = \frac{1}{2}I_{m3}\dot{\theta}_3^{\,2} k_r^2 + \frac{1}{2}m_{m3} v_2^T v_2$$

A further simplifying assumption is to consider the rotational kinetic energy of the motors to be a function only of the rotational velocities around their spinning axis. Indeed the off-diagonal elements in matrix $\Psi(q)$ are equal to zero.

$$T(q, \dot{q}, \dot{\theta}) = \begin{pmatrix} \dot{q}^T & \dot{\theta}^T \end{pmatrix} \Psi(q) \begin{pmatrix} \dot{q} \\ \dot{\theta} \end{pmatrix} = \begin{pmatrix} \dot{q}^T & \dot{\theta}^T \end{pmatrix} \begin{pmatrix} M(q) & 0 \\ 0 & B \end{pmatrix} \begin{pmatrix} \dot{q} \\ \dot{\theta} \end{pmatrix}$$

The parametrized inertia matrix will be given by:

$$M(q) = \begin{pmatrix} a_6 + 2a_2c_{23} + 2a_5c_2 + 2a_2c_3 & a_4 + a_3c_{23} + 2a_2c_3 + a_5c_2 & a_1 + a_2c_3 + a_3c_{23} \\ & a_4 + 2a_2c_3 & a_1 + a_2c_3 \\ symm & & a_1 \end{pmatrix}$$

Where:

$$a_1 = m_3 d_3^2 + I_3 \qquad a_2 = l_2 m_3 d_3$$
$$a_3 = d_3 l_1 m_3 \qquad a_4 = I_2 + I_2 + d_2^2 m_2 + d_3 m_3 + l_2^2 m_3 + l_2^2 m_{m3}$$
$$a_5 = m_2 l_1 d_2 + m_{m3} l_1 l_2 + m_3 l_1 l_2$$
$$a_6 = I_1 + I_2 + I_3 + d_1^2 m_1 + d_2^2 m_2 + d_3^2 m_3 + l_1^2 m_2 + l_1^2 m_3 + l_2^2 m_3 + l_1^2 m_{m2} + l_1^2 m_{m3} + l_2^2 m_{m3}$$

The motor inertia matrix is given by:

$$B = \begin{pmatrix} I_{m1}k_r^2 & 0 & 0 \\ 0 & I_{m2}k_r^2 & 0 \\ 0 & 0 & I_{m3}k_r^2 \end{pmatrix}$$

Then, each element of the centrifugal and Coriolis vector is computed as:

$$c_k(q, \dot{q}) = \dot{q}^T C_k \dot{q} \qquad where \;\; C_k = \frac{1}{2}\left(\frac{\partial m_k}{\partial q} + \left(\frac{\partial m_k}{\partial q}\right)^T - \frac{\partial M}{\partial q_k} \right)$$

Where m_k is the generic column of the inertia matrix $M(q)$.
The contribution of the potential energy can be computed as:

$$U_{el} = \frac{1}{2}(q - \theta)^T K (q - \theta)$$

Thus we will have:

$$\left(\frac{\partial U}{\partial z}\right)^T = \begin{pmatrix} K(q - \theta) \\ K(\theta - q) \end{pmatrix}$$

Finally we get the robot dynamic model:

$$M(q)\ddot{q} + c(q, \dot{q}) + K(q - \theta) = 0 \tag{1}$$
$$B\ddot{\theta} + K(\theta - q) = \tau \tag{2}$$

2.1 Torque as function of q and its derivatives

From (1) we can obtain θ as a function of q and its derivatives:

$$\theta = K^{-1}\big[M(q)\ddot{q} + c(q,\dot{q})\big] + q \tag{3}$$

We obtain $\ddot{\theta}$ by deriving twice (1):

$$\ddot{\theta} = K^{-1}\big[Mq^{(4)} + 2\dot{M}q^{(3)} + \ddot{M}\ddot{q} + \ddot{c}\big] + \ddot{q} \tag{4}$$

Substituting (3), (4) in (2), we obtain:

$$\tau = BK^{-1}\big[M(q)q^{(4)} + \alpha(q,\dot{q},\ddot{q},q^{(3)})\big]$$

2.2 Feedback

Since $\ddot{q}$ and $q^{(3)}$ are not easily measurable with sensors, we resort to measures of $(\theta,\dot{\theta},q,\dot{q})$, which can be measured accurately with encoders. Therefore we perform the change of coordinates by isolating $\ddot{q}$ and $q^{(3)}$ from (1) and its derivative:

$$\begin{aligned}\ddot{q} &= -M^{-1}\big[c(q,\dot{q}) + K(q-\theta)\big]\\ q^{(3)} &= -M^{-1}\big[\dot{M}\ddot{q} + \dot{c} + K(\dot{q}-\dot{\theta})\big]\end{aligned}$$

3 Local motor torque optimization

The Lagrange multipliers method is used. The cost index (5) is presented in the general form where τ_0 is a desired torque and W is a weight matrix which will be suitably selected. Furthermore, since the manipulator is required to perform a specific cartesian task, a kinematic constraint is presented:

$$H(\tau) = \frac{1}{2}(\tau - \tau_0)^T W (\tau - \tau_0) \tag{5}$$

$$Jq^{(4)} = p_d^{(4)} - \beta(\theta, \dot{\theta}, q, \dot{q}) \tag{6}$$

Where we will study six different scenarios as follows:

	$W = I$	$W = M^{-1}$	$W = M^{-2}$
$\tau_0 = 0$	A_1	B_1	C_1
$\tau_0 \neq 0$	A_2	B_2	C_2

The derivation of the previously presented kinematic constraint follows from the computation of derivatives of the EE position , up to the fourth order:

$$\begin{aligned}
\dot{p} &= Jq \\
\ddot{p} &= \dot{J}q + J\ddot{q} \\
p^{(3)} &= Jq^{(3)} + 2\dot{J}\ddot{q} + \ddot{J}\dot{q} \\
p^{(4)} &= Jq^{(4)} + 3\dot{J}q^{(3)} + \ddot{J}\ddot{q} + J^{(3)}\dot{q}
\end{aligned}$$

Then the constraint is represented from the last derivative.

$$\begin{aligned}
Jq^{4)} &= p^{(4)} - \beta(\theta, \dot{\theta}, q, \dot{q}) \\
\beta(\theta, \dot{\theta}, q, \dot{q}) &= 3\dot{J}q^{(3)} + \ddot{J}\ddot{q} + J^{(3)}\dot{q}
\end{aligned}$$

As a matter of fact, instead of setting $p^{(4)}$ as the fourth derivative of the desired trajectory $r(t)$, a more robust way of accomplishing the task is by performing a trajectory tracking. To this purpose a vector differential equation is set, whose objective is to let the cartesian error tend to zero as the task is performed:

$$p^{(4)} - r^{(4)} + K_3(p^{(3)} - r^{(3)}) + K_2(\ddot{p} - \ddot{r}) + K_1(\dot{p} - \dot{r}) + K_0(p - r) = 0$$

where K_i (for $i = 0, 1, 2, 3$) are chosen as diagonal, such that each row of the vector ζ is a Hurwitz polinomial.

$$\zeta(s) = s^4 + K_3\ s^3 + K_2\ s^2 + K_1\ s + K_0$$

Therefore, to render more efficient and robust the control law, the simulations will make use of this kinematic constraint:

$$\begin{aligned}
Jq^{4)} &= p^{(4)} - \beta(\theta, \dot{\theta}, q, \dot{q}) \\
p^{(4)} &= r^{(4)} - K_3\big[p^{(3)} - r^{(3)}\big] - K_2\big[\ddot{p} - \ddot{r}\big] - K_1\big[\dot{p} - \dot{r}\big] - K_0\big[p - r\big]
\end{aligned}$$

3.1 Stabilization in the null space

The vector τ_0 is introduced so to force a vector differential equation which aims, when possible, to reduce the values of the quantities $\dot{q}, \ddot{q}, q^{(3)}, q^{(4)}$:

$$\tau_0 = -\Gamma_1 \dot{q} - \Gamma_2 \ddot{q} - \Gamma_3 q^{(3)}$$
$$\gamma(s) = s^3 + \Gamma_3 s^2 + \Gamma_2 s + \Gamma_1$$

The vector $\Gamma(s)$ is chosen such that every component of the vector $\gamma(s)$ is Hurwitz. If the optimization procedure could ideally bring $\tau - \tau_0$ to zero, this relation would hold:

$$\tau - \tau_0 = 0$$
$$BK^{-1}\big[M(q)q^{(4)} + \alpha(q, \dot{q}, \ddot{q}, q^{(3)})\big] + \Gamma_3 q^{(3)} + \Gamma_2 \ddot{q} + \Gamma_1 \dot{q} = 0$$

This vector differential equation is indeed trying to force an attractive equilibrium point $(\dot{q}_{eq},\ \ddot{q}_{eq},\ q_{eq}^{(3)},\ q_{eq}^{(4)}) = (0, 0, 0, 0)$.

3.2 Case A_1

The derivation of the motor torque solution for the first case study is proved in the following.
The objective function takes the form:

$$H(q^{(4)}) = \frac{1}{2}\tau^T \tau = \frac{1}{2}\big[BK^{-1}(Mq^{(4)} + \alpha)\big]^T \big[BK^{-1}(Mq^{(4)} + \alpha)\big]$$

Define $A = BK^{-1}$ and rewrite $H(q^{(4)})$ as:

$$\begin{aligned} H(q^{(4)}) &= \frac{1}{2}\big[A(Mq^{(4)} + \alpha)\big]^T \big[A(Mq^{(4)} + \alpha)\big] = \\ &= \frac{1}{2}\big[q^{(4)^T} M^T A^T + \alpha^T A^T\big]\big[AMq^{(4)} + A\alpha\big] = \\ &= \frac{1}{2}\big[q^{(4)^T} MA^2Mq^{(4)} + \alpha^T A^2 \alpha + 2\alpha^T A^2 M q^{(4)}\big] \end{aligned}$$

Now define the Lagrangian function:

$$\mathcal{L} = \frac{1}{2}\big[q^{(4)^T}(MA^2M)q^{(4)} + \alpha^T A^2 \alpha + 2\alpha^T A^2 M q^{(4)}\big] + \lambda(Jq^{(4)} - y)$$

and impose:

$$\frac{\partial \mathcal{L}}{\partial q^{(4)}} = 0 \qquad \frac{\partial \mathcal{L}}{\partial \lambda} = 0$$

yielding:

$$\left(\frac{\partial \mathcal{L}}{\partial q^{(4)}}\right)^T = (MA^2M)q^4 + MA^2\alpha + J^T\lambda = 0$$

Isolate $q^{(4)}$:

$$q^4 = -(MA^2M)^{-1}\big[MA^2\alpha + J^T\lambda\big]$$

and substitute it in the constraint (6):

$$J(MA^2M)^{-1}\big[MA^2\alpha + J^T\lambda\big] + y = 0$$

Therefore we have that:

$$\begin{aligned}\big((MA^2M)^{-1}J^T\big)\lambda &= -y - J(MA^2M)^{-1}MA^2\alpha \\ \lambda &= -\big((MA^2M)^{-1}J^T\big)^{-1} \\ q^{(4)} &= -(I - J_\Omega^{\#}J)M^{-1}\alpha + J_\Omega^{\#}y\end{aligned}$$

where:

$$\begin{aligned}\Omega &= MA^2M \\ J_\Omega^{\#} &= \Omega^{-1}J^T(J\Omega^{-1}J^T)^{-1}\end{aligned}$$

3.3 Case A_2

This case study aims at minimizing the error between the motor torque with respect to a desired one, which aims at stabilizing the robot and has the effect of reducing oscillatory movements:

$$\begin{aligned}H(\tau) = \frac{1}{2}(\tau - \tau_0)^T(\tau - \tau_0) = \\ = \frac{1}{2}q^{(4)^T}(MA^2M)q^{(4)} + \frac{1}{2}\alpha^TA^2\alpha + \alpha^TA^2Mq^{(4)} + \\ + \frac{1}{2}\tau_0^TA^2\tau_0 - \tau_0^TA\big[Mq^{(4)} + \alpha\big]\end{aligned}$$

Construct the Lagrangian function:

$$\begin{aligned}\mathcal{L} &= H + \lambda^T(Jq^{(4)} - y) \\ \frac{\partial\mathcal{L}}{\partial q^{(4)}} &= MA^2Mq^{(4)} + MA^2\alpha - MA\tau_0 + J^T\lambda = 0 \\ q^{(4)} &= M^{-1}A^{-1}\tau_0 - M^{-1}\alpha - (MA^2M)^{-1}J^T\lambda\end{aligned}$$

Substitute in the constraint (6) in order to obtain the lagrangian multipliers, yielding the optimal solution $q^{(4)}$:

$$\begin{aligned}\lambda &= (J(MA^2M)^{-1}J^T)^{-1}(JM^{-1}A^{-1}\tau_0 - JM^{-1}\alpha - y) \\ q^{(4)} &= (I - J_\Omega^{\#}J)M^{-1}A^{-1}\tau_0 - (I - J_\Omega^{\#}J)M^{-1}\alpha + J_\Omega^{\#}y\end{aligned}$$

Since the weighted pseudoinverse satisfies the property:

$$J(I - J_\Omega^{\#}J) = 0$$

Thus, the vector τ_0 is projected into the null space $\mathcal{N}(J)$, and therefore has no influence at all on the constraint (6).

3.4 Case B_1

Since the first joint of the robot perceives a greater inertia wrt the others, it follows that if a different weight is not assigned to the three torques into the control law, then the first link will necessarily perform a smaller movement.
Therefore the cost index is modified as follows:

$$H(\tau) = \frac{1}{2}\tau^T M^{-1}\tau =$$
$$= \frac{1}{2}\left[BK^{-1}(Mq^{(4)} + \alpha)\right]^T M^{-1}\left[BK^{-1}(Mq^{(4)} + \alpha)\right] =$$
$$= \frac{1}{2}q^{(4)T}(MK^{-1}BM^{-1}BK^{-1}M)q^{(4)} + \alpha^T(K^{-1}BM^{-1}BK^{-1}M)q^{(4)} +$$
$$+ \frac{1}{2}\alpha^T(K^{-1}BM^{-1}BK^{-1})\alpha$$

But thanks to the fact that both the elastic constant and the reduction ratio of each motor are chosen equal, the matrices K, B are just scaled identity matrices. This means that the product with this matrices commutes:

$$MK^{-1}BM^{-1}BK^{-1}M = MK^{-2}B^2 = MA^2$$
$$K^{-1}BM^{-1}BK^{-1}M = A^2$$

Where the matrix $A = K^{-1}B$. Similarly to the previous cases, the Lagrange multipliers method is applied, yielding the optimal solution:

$$\mathcal{L} = \frac{1}{2}\left[q^{(4)T}(MA^2)q^{(4)} + \alpha^T M^{-1}A^2\alpha + 2\alpha^T A^2 q^{(4)}\right] + \lambda(Jq^{(4)} - y)$$

Then by equating the derivative w.r.t. $q^{(4)}$ to zero and isolating $q^{(4)}$ we get:

$$\frac{\partial \mathcal{L}}{\partial q^{(4)}} = MA^2q^4 + A^2\alpha + J^T\lambda = 0$$
$$q^4 = -M^{-1}\alpha - M^{-1}A^{-2}J^T\lambda$$

By substituting this result in the constraint equation (6) the expression for λ and q^4 can be obtained:

$$-JM^{-1}A^{-2}J^T\lambda - JM^{-1}\alpha - y = 0$$
$$\lambda = -\left(JM^{-1}A^{-2}J^T\right)^{-1}\left(JM^{-1}\alpha + y\right)$$
$$q^{(4)} = -\left(I - J_M^{\#}J\right)M^{-1}\alpha + J_M^{\#}y$$

Moreover the torque takes the form:

$$\tau = AJ^T\left(JM^{-1}J^T\right)^{-1}\left(JM^{-1}\alpha + y\right)$$

This expression is dynamically consistent since presents a scaled Jacobian matrix to the left of the expression.

3.5 Case B_2

Analogously to case A, a stabilization in the null space is introduced, and thus the cost index rewrites as:

$$
\begin{gathered}
H(\tau) = \frac{1}{2}(\tau - \tau_0)^T M^{-1}(\tau - \tau_0) = \\
= \frac{1}{2}\big[BK^{-1}(Mq^{(4)} + \alpha) - \tau_0\big]^T M^{-1}\big[BK^{-1}(Mq^{(4)} + \alpha)\big] = \\
= \frac{1}{2}q^{(4)T}(MK^{-1}BM^{-1}BK^{-1}M)q^{(4)} + \alpha^T(K^{-1}BM^{-1}BK^{-1}M)q^{(4)} + \\
+ \frac{1}{2}\alpha^T(K^{-1}BM^{-1}BK^{-1})\alpha - \tau_0^T Aq^{(4)} - \tau_0 M^{-1}A\alpha + \frac{1}{2}\tau_0^T M^{-1}\tau_0
\end{gathered}
$$

By using the same procedure as before:

$$
\begin{gathered}
q^{(4)} = -M^{-1}\alpha - M^{-1}A^{-2}J^T\lambda + M^{-1}A^{-1}\tau_0 \\
\lambda = \big(JM^{-1}A^{-2}J^T\big)^{-1}\big(-JM^{-1}\alpha - y + JM^{-1}A^{-1}\tau_0\big)
\end{gathered}
$$

Then by combining the two previous relations the optimal result is obtained:

$$
q^{(4)} = -\big(I - J_M^{\#}J\big)M^{-1}\alpha + J_M^{\#}y + \big(I - J_M^{\#}J\big)M^{-1}A^{-1}\tau_0
$$

Moreover the torque takes the form:

$$
\tau = AJ^T\big(JM^{-1}J^T\big)^{-1}\big(JM^{-1}\alpha + y\big) + (I - J^T(JM^{-1}J^T)^{-1}JM^{-1})\tau_0
$$

3.6 Case C_1

An even more effective weighting matrix can be chosen as the square of the inertia matrix. Indeed, this solution yields a better performance and is to be preferred. The new cost index is written as follows:

$$
\begin{gathered}
H(\tau) = \frac{1}{2}\tau^T M^{-2}\tau = \\
= \frac{1}{2}q^{(4)T}(MK^{-1}BM^{-2}BK^{-1}M)q^{(4)} + \alpha^T(K^{-1}BM^{-2}BK^{-1}M)q^{(4)} + \\
+ \frac{1}{2}\alpha^T(K^{-1}BM^{-2}BK^{-1})\alpha = \\
= \frac{1}{2}q^{(4)T}A^2q^{(4)} + \frac{1}{2}\alpha^T M^{-2}A^2\alpha + \alpha^T A^2 M^{-1}q^{(4)}
\end{gathered}
$$

The optimal solution is computed as in previous cases as:

$$
\begin{gathered}
\lambda = -\big(JA^{-2}J^T\big)^{-1}\big(JM^{-1}\alpha + y\big) \\
q^{(4)} = -M^{-1}\alpha - A^{-2}J^T\lambda
\end{gathered}
$$

By combining the last two equations:

$$
\begin{gathered}
q^{(4)} = -\big(I - J^{\#}J\big)M^{-1}\alpha + J^{\#}y \\
\tau = AMJ^{\#}\big(JM^{-1}\alpha + y\big)
\end{gathered}
$$

3.7 Case C_2

As previously, a stabilization in the null space is introduced, and thus the cost index rewrites as:

$$
\begin{gathered}
H(\tau) = \frac{1}{2}(\tau - \tau_0)^T M^{-2}(\tau - \tau_0) = \\
= \frac{1}{2}q^{(4)T} A^2 q^{(4)} + \frac{1}{2}\alpha^T M^{-2} A^2 \alpha + \alpha^T A^2 M^{-1} q^{(4)} + \\
-\tau_0^T M^{-1} A q^{(4)} - \tau_0^T M^{-2} A \alpha + \frac{1}{2}\tau_0^T M^{-2} \tau_0
\end{gathered}
$$

The optimal solution is given by:

$$
\begin{gathered}
\lambda = \big(JA^{-2}J^T\big)^{-1}\big(- JM^{-1}\alpha - y + JM^{-1}A^{-1}\tau_0\big) \\
q^{(4)} = -M^{-1}\alpha - A^{-2}J^T\lambda + A^{-1}M^{-1}\tau_0
\end{gathered}
$$

By combining the last two equations:

$$
\begin{gathered}
q^{(4)} = -\big(I - J^{\#}J\big)M^{-1}\alpha + J^{\#}y + \big(I - J^{\#}J\big)A^{-1}M^{-1}\tau_0 \\
\tau = AMJ^{\#}\big(JM^{-1}\alpha + y) + M(I - JJ^{\#})M^{-1}\tau_0
\end{gathered}
$$

4 Simulations

A normalized polynomial of 7^{th} degree is defined, satisfying a rest to rest trajectory, both in the linear and circular trajectories cases, as follows:

$$
\begin{aligned}
s(t) &= h\Bigg[-20\Big(\frac{t}{T}\Big)^7+70\Big(\frac{t}{T}\Big)^6-84\Big(\frac{t}{T}\Big)^5+35\Big(\frac{t}{T}\Big)^4\Bigg]\\
\dot{s}(t) &= \Big(\frac{140h}{T}\Big)\Bigg[-\Big(\frac{t}{T}\Big)^6+3\Big(\frac{t}{T}\Big)^5-3\Big(\frac{t}{T}\Big)^4+\Big(\frac{t}{T}\Big)^3\Bigg]\\
\ddot{s}(t) &= \Big(\frac{420h}{T^2}\Big)\Bigg[-2\Big(\frac{t}{T}\Big)^5+5\Big(\frac{t}{T}\Big)^4-4\Big(\frac{t}{T}\Big)^3+\Big(\frac{t}{T}\Big)^2\Bigg]\\
\dddot{s}(t) &= \Big(\frac{840h}{T^3}\Big)\Bigg[-5\Big(\frac{t}{T}\Big)^4+10\Big(\frac{t}{T}\Big)^3-6\Big(\frac{t}{T}\Big)^2+\Big(\frac{t}{T}\Big)\Bigg]\\
s^{(4)}(t) &= \Big(\frac{840h}{T^4}\Big)\Bigg[-20\Big(\frac{t}{T}\Big)^3+30\Big(\frac{t}{T}\Big)^2-12\Big(\frac{t}{T}\Big)+1\Bigg]
\end{aligned}
$$

The robot data are the following:

- Link mass: $m_i = 10Kg$
- Motor mass: $m_{mi} = 1Kg$
- Link moment of inertia: $I_i = 3.33Kgm^2$
- Motor moment of inertia: $m_i = 0.01Kgm^2$
- Link lenght: $l_i = 1m$
- Distance between joints and centers of masses: $d_i = 0.5m$
- Reduction ratio: $k_r = 100$
- Elastic constant: $K = 1000N/m$

4.1 Linear trajectory

The results of the Matlab and Simulink simulations with a linear trajectory are shown and analyzed in the following. In particular, there will be a focus in comparing the results with $\tau_0 = 0$ and with $\tau_0 \neq 0$, in order to study the effects of stabilization in the null space.
For each choice of the weighting matrix, in the following are shown the stroboscopic views of the robot movements, the graphs of joint accelerations and velocities, and the plots of the error $q - \theta$. The simulation is defined as follows:

- Simulation time $T = 2.58$, simulation time $T_s = 0.01$
- Initial point: [1.41;-0.41], final point: [1.41;0.41]

- Initial configuration: $\left[-\frac{\pi}{4};\frac{3\pi}{4};-\frac{3\pi}{4}\right]$
- Trajectories definition:

$$p_d(t) = p_{in} + \left(\frac{s}{||p_{fin} - p_{in}||}\right)(p_{fin} - p_{in})$$
$$\dot{p_d}(t) = \left(\frac{\dot{s}}{||p_{fin} - p_{in}||}\right)(p_{fin} - p_{in})$$
$$\ddot{p_d}(t) = \left(\frac{\ddot{s}}{||p_{fin} - p_{in}||}\right)(p_{fin} - p_{in})$$
$$\dddot{p_d}(t) = \left(\frac{\dddot{s}}{||p_{fin} - p_{in}||}\right)(p_{fin} - p_{in})$$
$$p_d^{(4)}(t) = \left(\frac{s^{(4)}}{||p_{fin} - p_{in}||}\right)(p_{fin} - p_{in})$$

4.1.1 Cases A_1 , A_2

Performances with $W = I$. The stabilization in the null space is done through the following τ_0 which corresponds to a desired polynomial $(s+5)^3$:

$$\tau_0 = -125\ \dot{q} - 75\ \ddot{q} - 15\ \dddot{q}$$

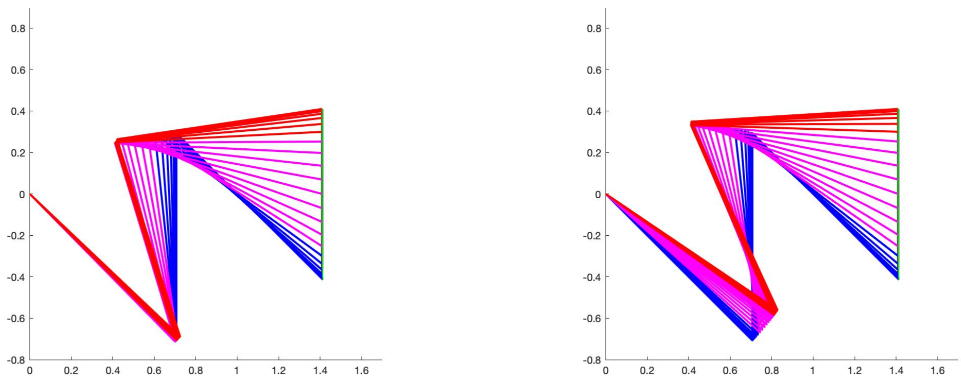

(a) Case A_1 : $\tau_0 = 0$

(b) Case A_2 : $\tau_0 \neq 0$

Figure 1: Stroboscopic view

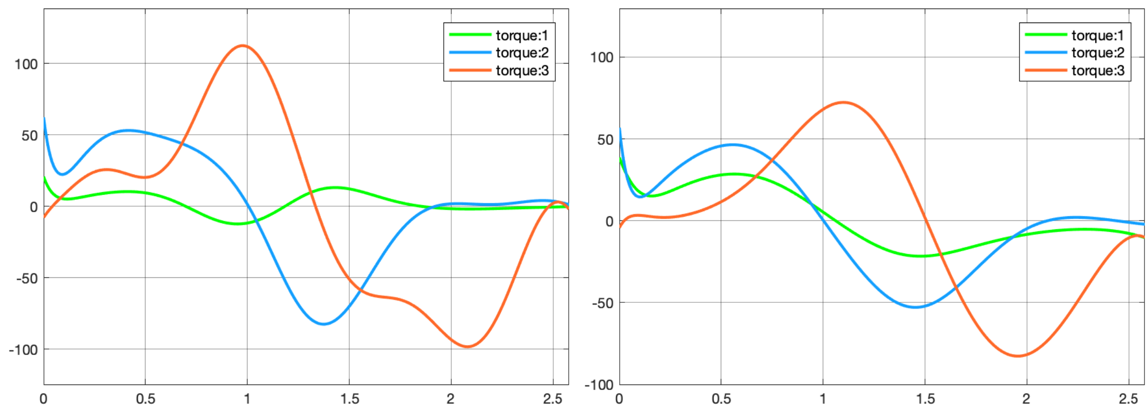

(a) Case A_1 : $\tau_0 = 0$ (b) Case A_2 : $\tau_0 \neq 0$

Figure 2: Motor torques

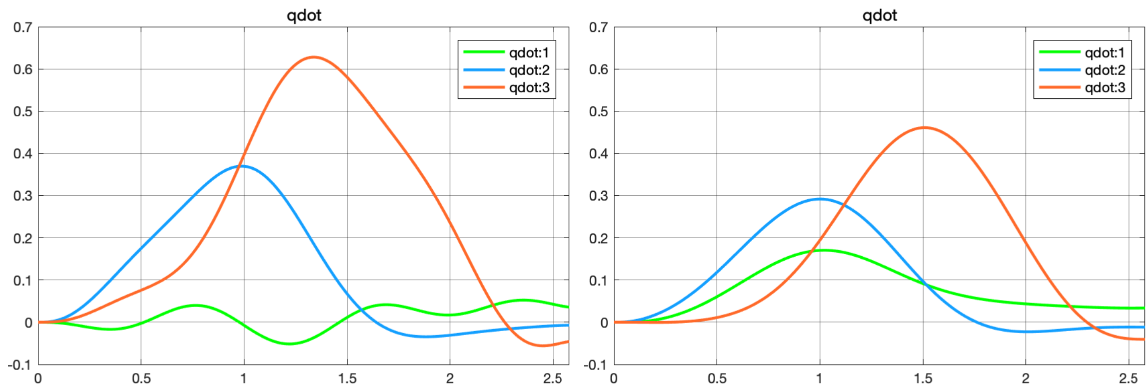

(a) Case A_1 : $\tau_0 = 0$ (b) Case A_2 : $\tau_0 \neq 0$

Figure 3: Joint velocities

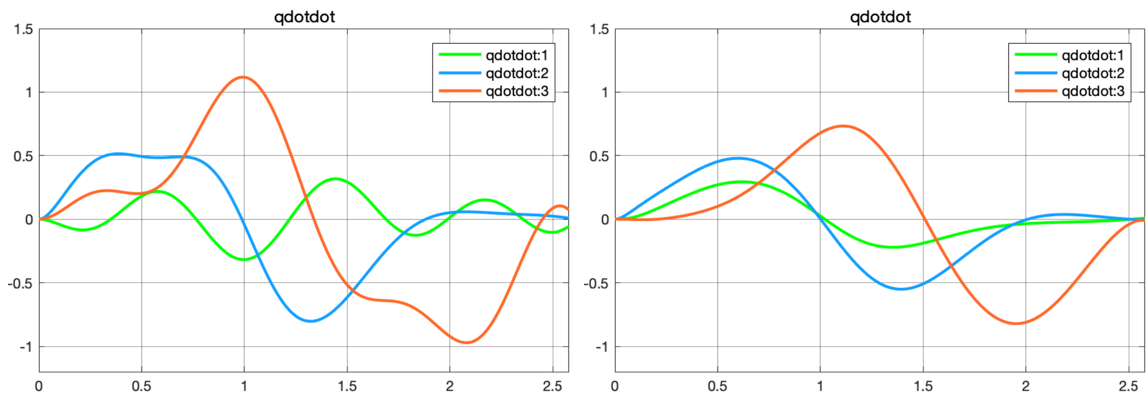

(a) Case A_1 : $\tau_0 = 0$ (b) Case A_2 : $\tau_0 \neq 0$

Figure 4: Joint accelerations

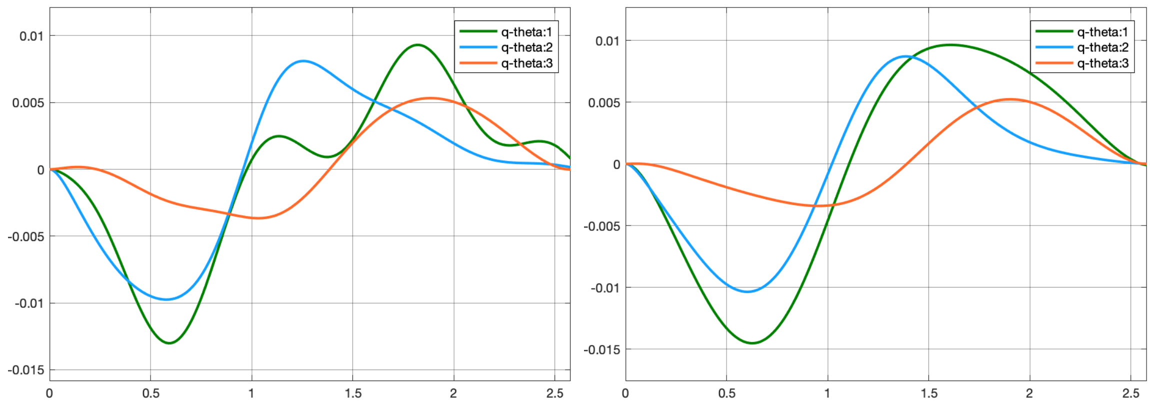

(a) Case $A_1 : \tau_0 = 0$ (b) Case $A_2 : \tau_0 \neq 0$

Figure 5: Error $q - \theta$

It is possible to notice that in the case with $W = I$, the stabilization in the null space offers a better optimization: indeed less motor torques are used, while the values of the error $q - \theta$ are similar.

4.1.2 Cases B_1, B_2

Performances with $W = M^{-1}$. The stabilization in the null space is done through the following τ_0, which corresponds to the polynomial $(s + 20)^3$:

$$\tau_0 = -8000\ \dot{q} - 1200\ \ddot{q} - 60\ \dddot{q}$$

In this case, in order to render the evolution smoother, the roots of the polynomial have been chosen in -20 while for case A_2 roots in -5 were enough to avoid oscillations.

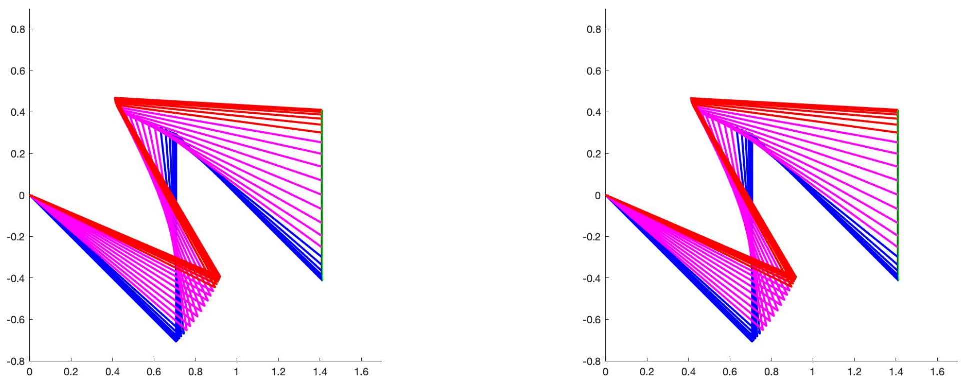

(a) Case $B_1 : \tau_0 = 0$ (b) Case $B_2 : \tau_0 \neq 0$

Figure 6: Stroboscopic view

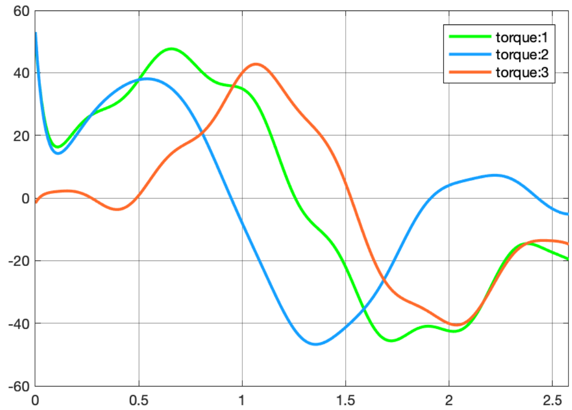

(a) Case $B_1 : \tau_0 = 0$

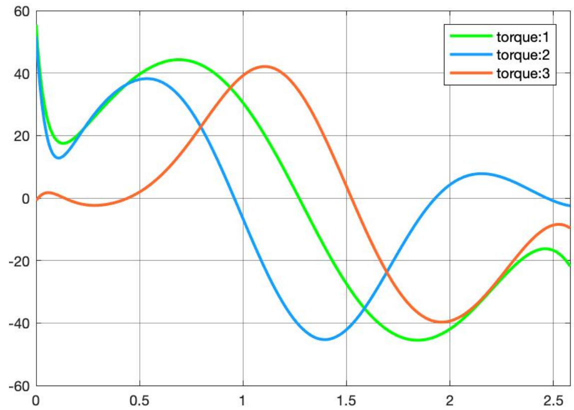

(b) Case $B_2 : \tau_0 \neq 0$

Figure 7: Motor toruqes

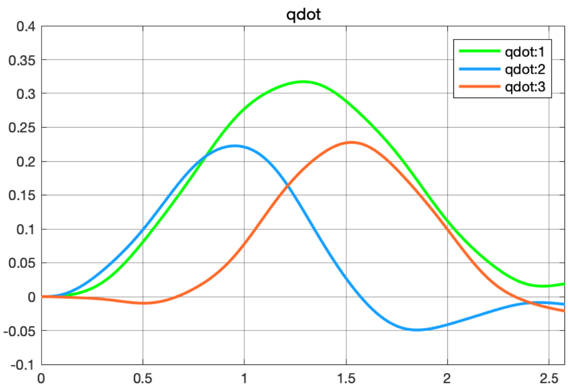

(a) Case $B_1 : \tau_0 = 0$

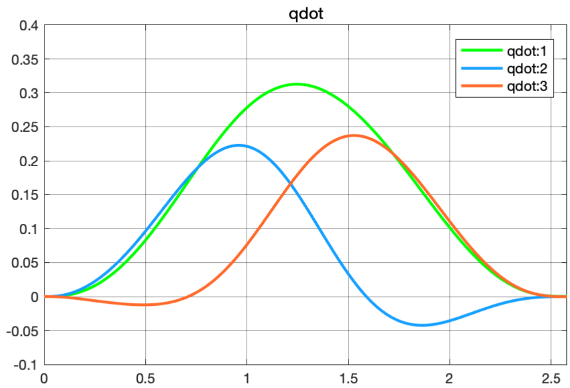

(b) Case $B_2 : \tau_0 \neq 0$

Figure 8: Joint velocities

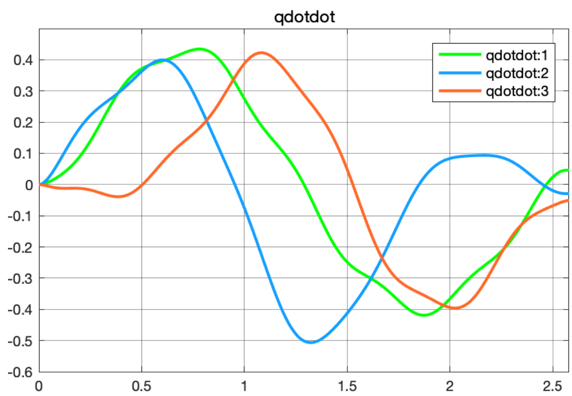

(a) Case $B_1 : \tau_0 = 0$

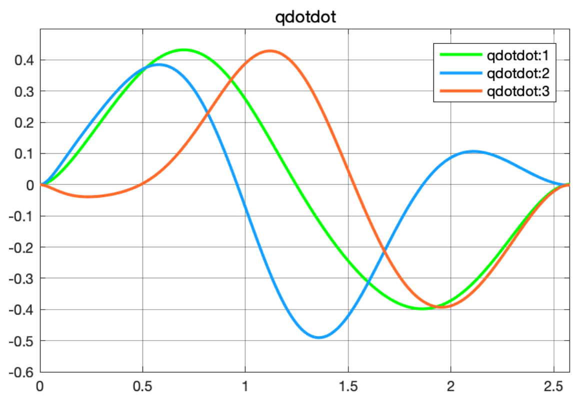

(b) Case $B_2 : \tau_0 \neq 0$

Figure 9: Joint accelerations

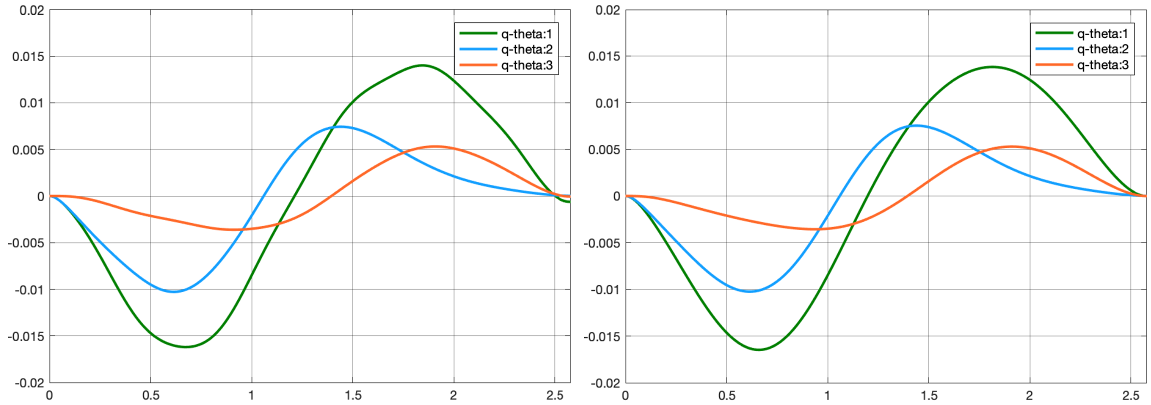

(a) Case $B_1 : \tau_0 = 0$ (b) Case $B_2 : \tau_0 \neq 0$

Figure 10: Error $q - \theta$

It is possible to notice that the first joint performs broader movements with respect to case A, and this is because since the inertia perceived by the first joint is greater than the other two, and since the weighting matrix is now $W = M^{-1}$, we have as a result a lower weight on the torque exerted by joint one. Moreover, the results obtained with $W = M^{-1}$ display significantly reduced motor torques with respect to case A. Therefore the use of the inverse of the inertia matrix M yields a better optimization performance.

4.1.3 Cases C_1, C_2

Performances with $W = M^{-2}$. The stabilization in the null space is done through the following τ_0, which corresponds to the polynomial $(s + 5)^3$:

$$\tau_0 = -125\ \dot{q} - 75\ \ddot{q} - 15\ \dddot{q}$$

For this specific path, the choice for the weighting M^{-2} causes the evolution in case C_1 to be smoother than the one in B_1, therefore in this case it is not necessary to force a very reactive τ_0 such as in case B_2. The addition of the stabilization in the null space has the effect of reducing the torque exerted by motor 3 while requesting more effort from motor 1.

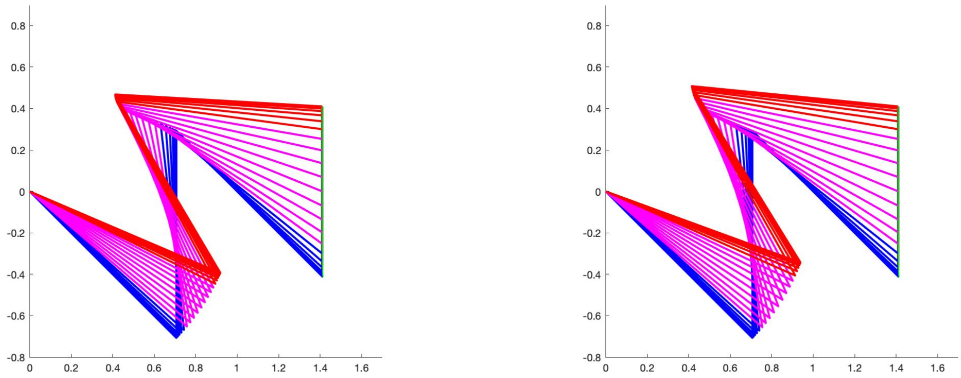

(a) Case $C_1 : \tau_0 = 0$ (b) Case $C_2 : \tau_0 \neq 0$

Figure 11: Stroboscopic view

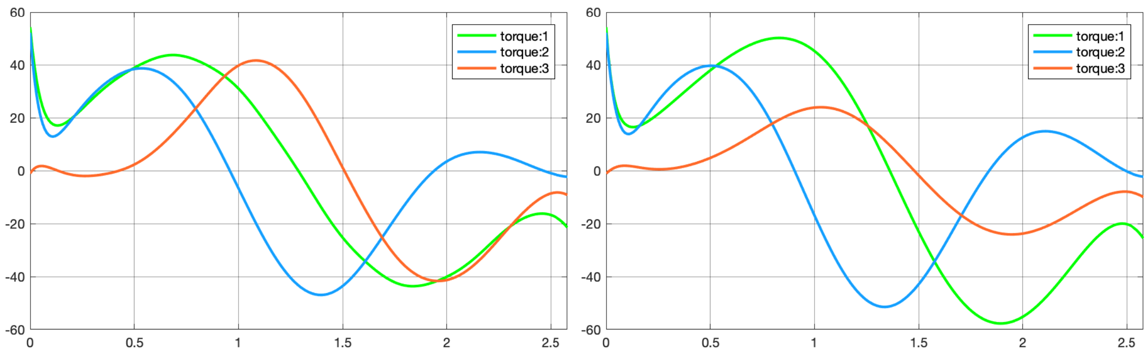

(a) Case $C_1 : \tau_0 = 0$ (b) Case $C_2 : \tau_0 \neq 0$

Figure 12: Motor torques

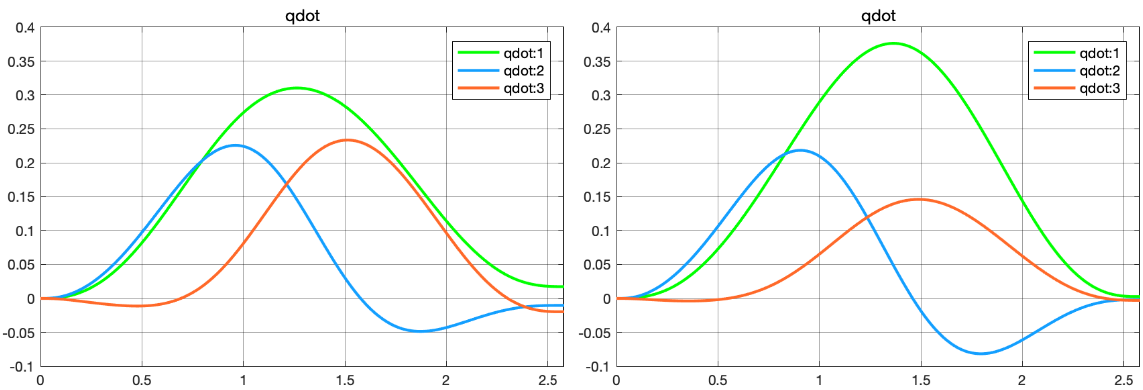

(a) Case $C_1 : \tau_0 = 0$ (b) Case $C_2 : \tau_0 \neq 0$

Figure 13: Joint velocities

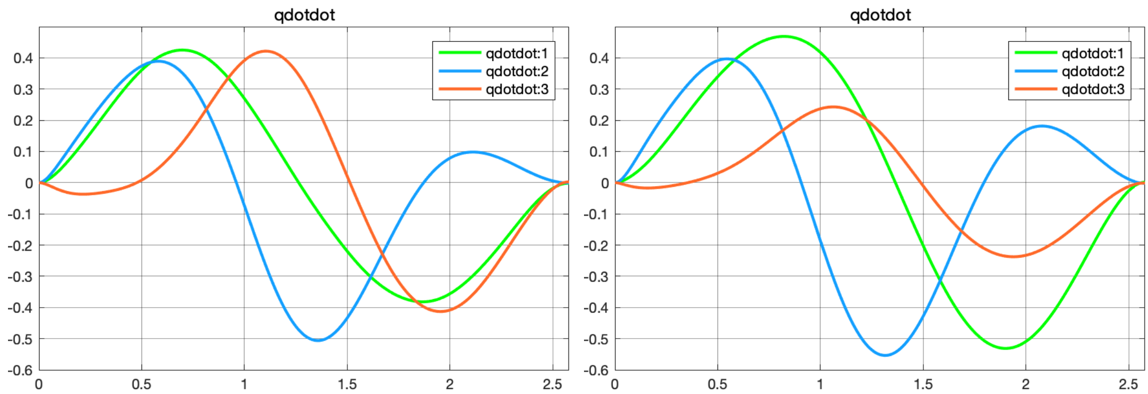

(a) Case $C_1 : \tau_0 = 0$ (b) Case $C_2 : \tau_0 \neq 0$

Figure 14: Joint accelerations

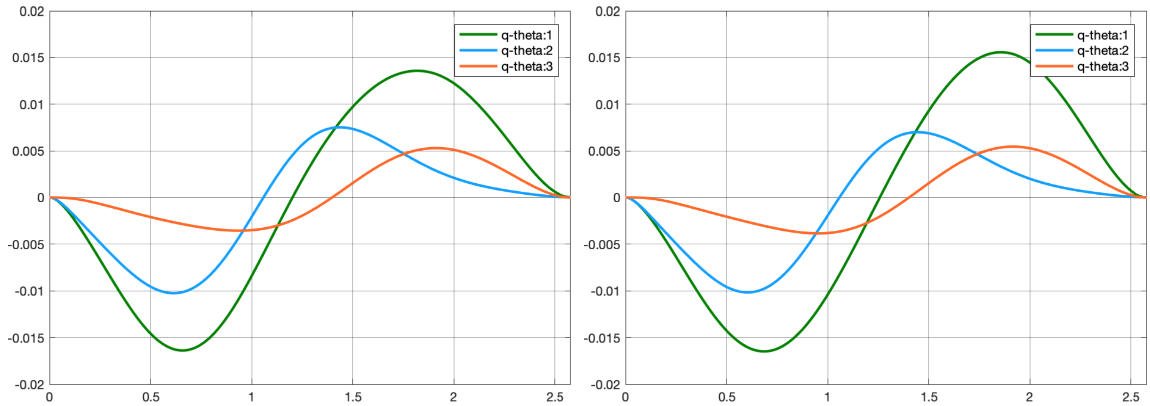

(a) Case $C_1 : \tau_0 = 0$ (b) Case $C_2 : \tau_0 \neq 0$

Figure 15: Error $q - \theta$

The robot motion is still more fluid in this case, as it is possible to see in the animations. This is due to the choice of $W = M^{-2}$ as weighting matrix, yielding a better optimization performance.

4.2 Circular trajectory

Now the results of the Matlab and Simulink simulations with a circular trajectory are shown and analyzed. Also in this case, there will be a special focus in comparing the results with $\tau_0 = 0$ and with $\tau_0 \neq 0$, in order to study the influence of stabilization in the null space.

The simulations are performed on the same trajectory and have same initial configuration whereas the simulation time varies between $T = 20s$ and $T = 10s$. The longer simulation time aims at showing that the robot is able to perform a good trajectory tracking, with an error of 0.5 mm on a circumference of diameter 80 cm. This result is shown in the partial stroboscopic view of each case. As a matter of fact this longer time does not allow oscillations to occur, therefore the effect of the Stabilization in the null space is not evident. On the contrary if a shorter time of $10s$ is chosen,the stabilization can help to remove some unwanted oscillatory behaviour. The price to pay for reducing the task execution time is that in this case the robot commits almost a 2 cm error on the same path.

- Simulation time $T_{long} = 20$,$T_{short} = 10$. Sampling time $T_s = 0.01$
- Initial configuration: $[\pi; -\frac{\pi}{2}; -\frac{\pi}{2}]$
- Radius: $R = 0.4$
- Trajectories definition:

$$p_d = \begin{pmatrix} Rcos(s) + x_0 \\ Rsin(s) + y_0 \end{pmatrix}$$

$$\dot{p_d} = \begin{pmatrix} -Rsin(s)\dot{s} \\ Rcos(s)\dot{s} \end{pmatrix}$$

$$\ddot{p_d} = \begin{pmatrix} -Rcos(s)\dot{s}^2 - Rsin(s)\ddot{s} \\ -Rsin(s)\dot{s}^2 + Rcos(s)\ddot{s} \end{pmatrix}$$

$$\dddot{p_d} = \begin{pmatrix} -Rsin(s)\dot{s}^3 - Rsin(s)\dddot{s} - 3Rcos(s)\ddot{s}\dot{s} \\ -Rcos(s)\dot{s}^3 - Rcos(s)\dddot{s} - 3Rsin(s)\ddot{s}\dot{s} \end{pmatrix}$$

$$p_d^{(4)} = \begin{pmatrix} Rcos(s)\dot{s}^4 - 3Rcos(s)\ddot{s}^2 - Rsin(s)s^{(4)} + 6Rsin(s)\ddot{s}\dot{s}^2 - 4Rcos(s)\dddot{s}\,\dot{s} \\ Rsin(s)\dot{s}^4 - 3Rsin(s)\ddot{s}^2 + Rcos(s)s^{(4)} - 6Rsin(s)\ddot{s}\dot{s}^2 - 4Rsin(s)\dddot{s}\,\dot{s} \end{pmatrix}$$

4.2.1 Cases A_1A_2

Performances with $W = I$.

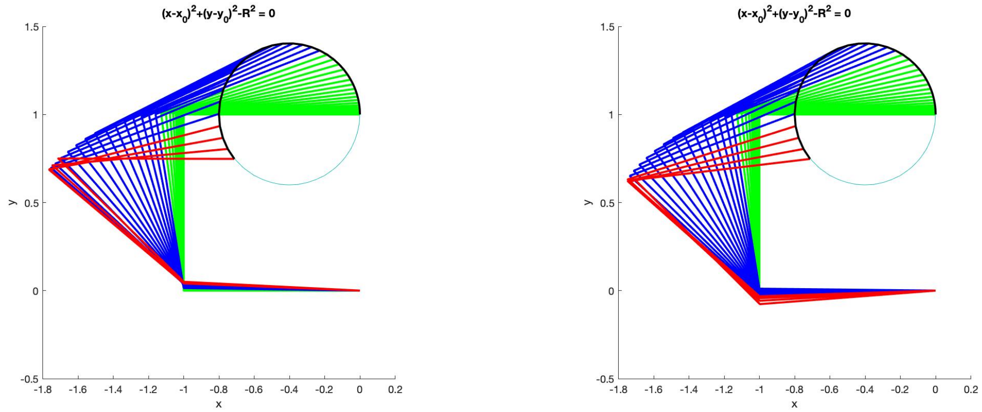

(a) Case $A_1 : \tau_0 = 0$ (b) Case $A_2 : \tau_0 \neq 0$

Figure 16: Partial stroboscopic view , T_{long}

The stroboscopic view show only a part of the robot movement for graphic reasons. The absence of the weighting matrix in the objective function renders the system subject to unwanted oscillatory behaviour, as shown in fig. 17 (a) even with the longer simulation time $T_{long} = 20\ s$

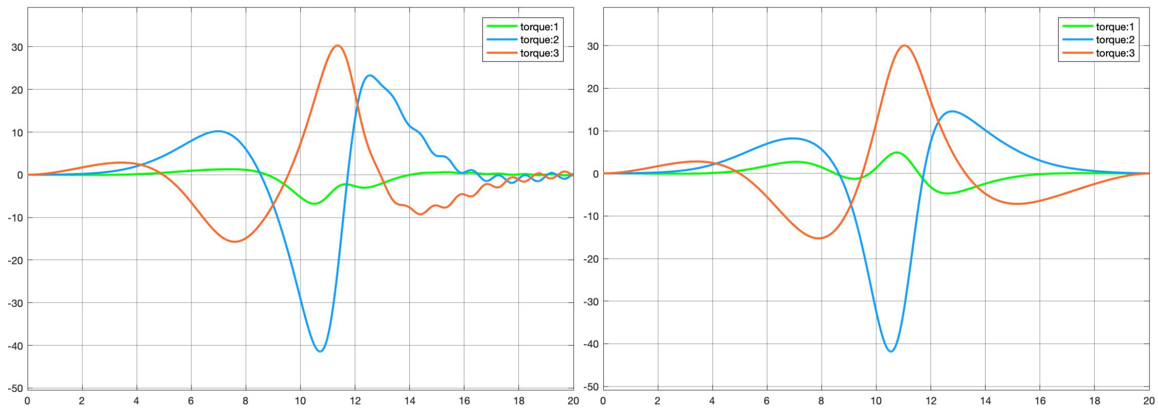

(a) Case $A_1 : \tau_0 = 0$ (b) Case $A_2 : \tau_0 \neq 0$

Figure 17: Motor torques , T_{long}

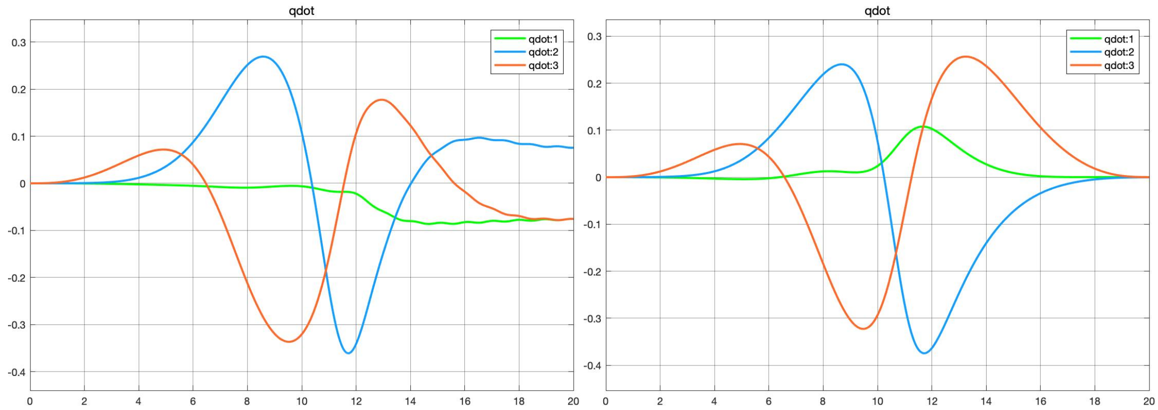

(a) Case $A_1 : \tau_0 = 0$ (b) Case $A_2 : \tau_0 \neq 0$

Figure 18: Joint velocities , T_{long}

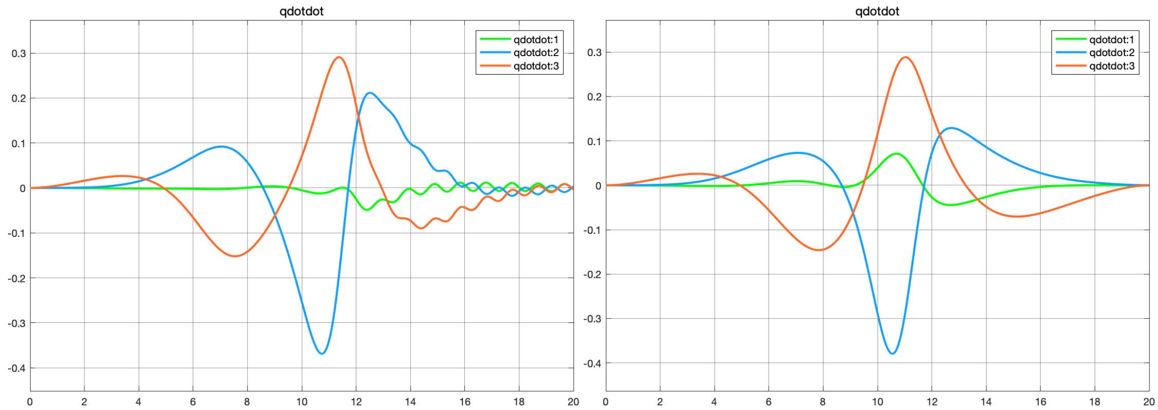

(a) Case $A_1 : \tau_0 = 0$ (b) Case $A_2 : \tau_0 \neq 0$

Figure 19: Joint accelerations , T_{long}

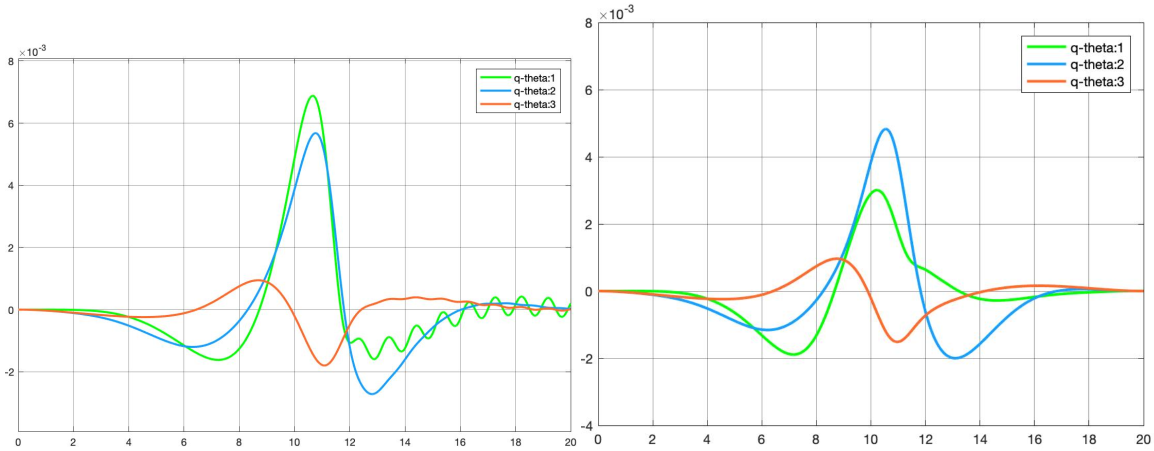

(a) Case $A_1 : \tau_0 = 0$ (b) Case $A_2 : \tau_0 \neq 0$

Figure 20: Error $q - \theta$, T_{long}

It is possible to notice that in the case with $W = I$, the stabilization in the null space avoids oscillations and lowers the values of the error $q - \theta$.

4.2.2 Cases $B_1 B_2$

Performances with $W = M^{-1}$.

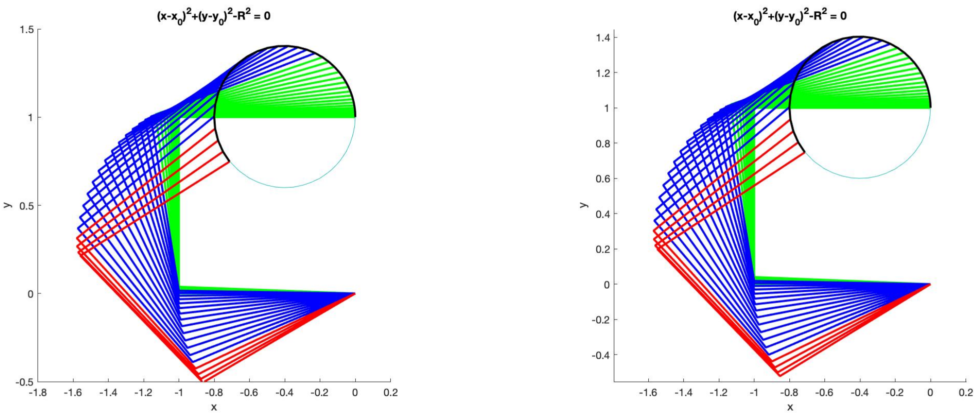

(a) Case $B_1 : \tau_0 = 0$ (b) Case $B_2 : \tau_0 \neq 0$

Figure 21: Partial stroboscopic view , T_{long}

In this case the reduction of the simulation time from $T_{long} = 20\ s$ to $T_{short} = 10\ s$ was necessary to show the effectiveness of stabilizing in the null space.

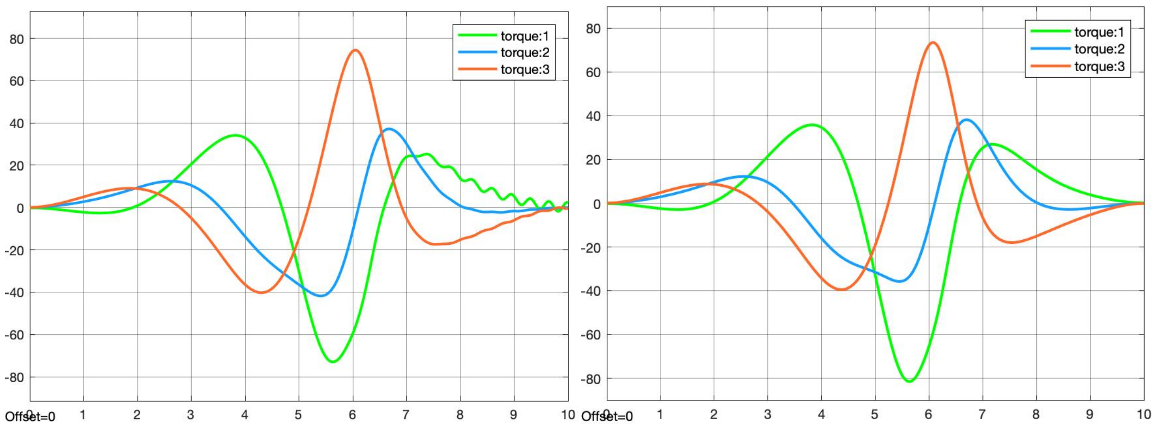

(a) Case $B_1 : \tau_0 = 0$ (b) Case $B_2 : \tau_0 \neq 0$

Figure 22: Motor torques , T_{short}

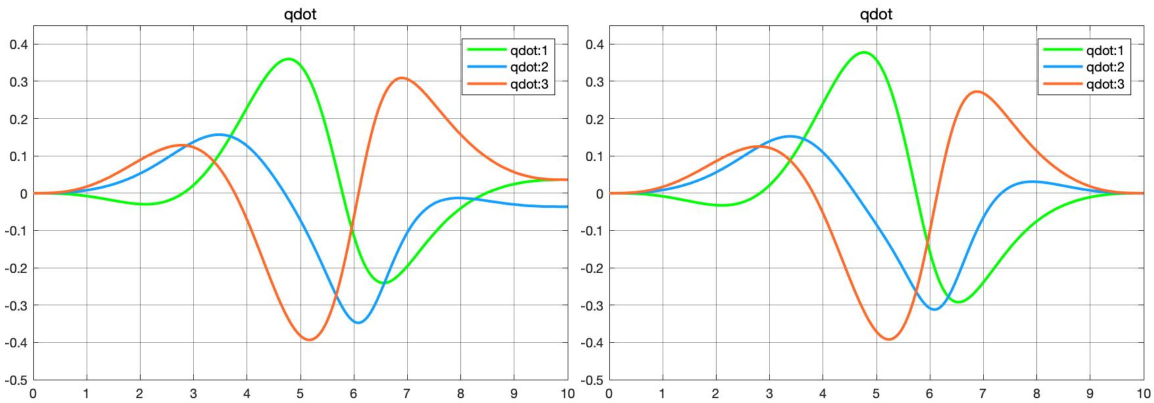

(a) Case $B_1 : \tau_0 = 0$ (b) Case $B_2 : \tau_0 \neq 0$

Figure 23: Joint velocities, T_{short}

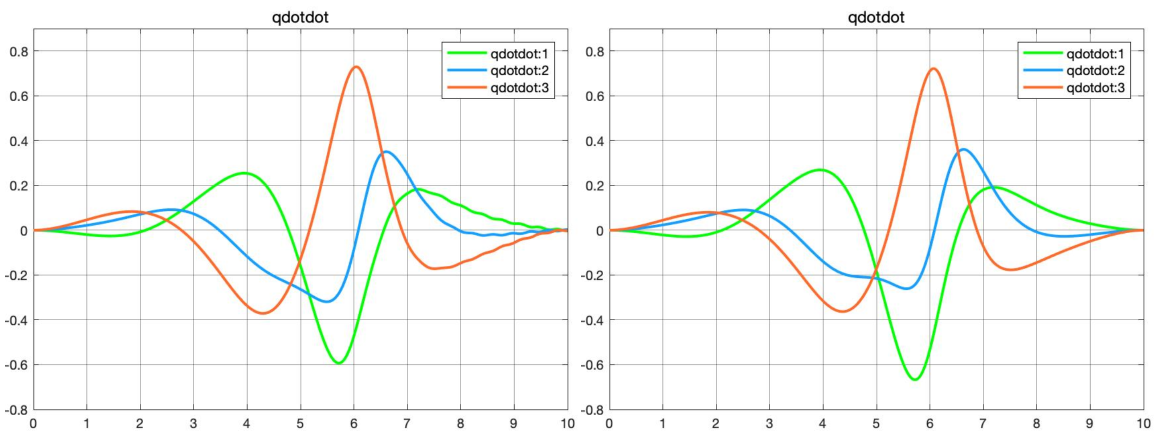

(a) Case $B_1 : \tau_0 = 0$ (b) Case $B_2 : \tau_0 \neq 0$

Figure 24: Joint accelerations , T_{short}

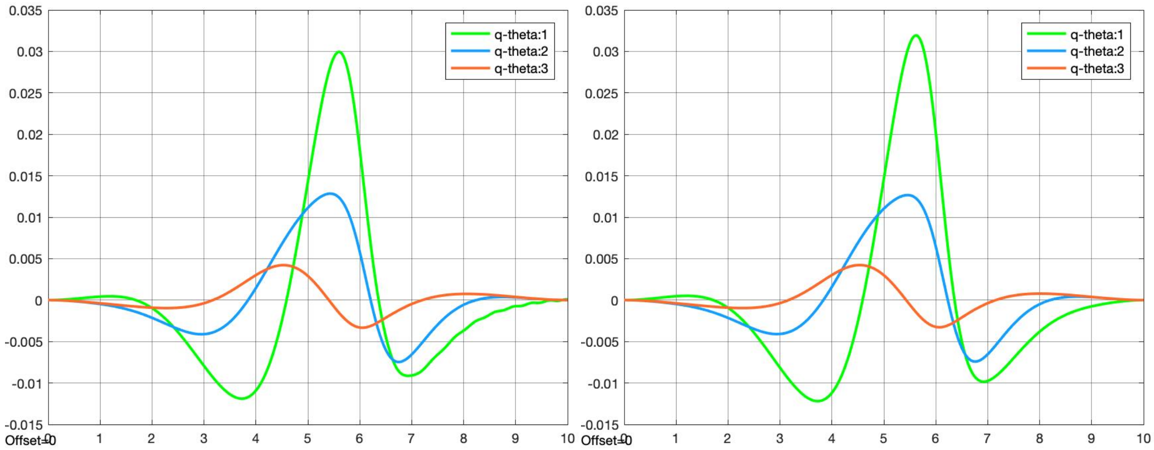

(a) Case $B_1 : \tau_0 = 0$ (b) Case $B_2 : \tau_0 \neq 0$

Figure 25: Error $q - \theta$, T_{short}

The results obtained with $W = M^{-1}$ display significantly reduced motor torques with respect to case A. Therefore the use of the inverse of the inertia matrix M yields a better optimization performance.

4.2.3 Cases C_1C_2

Performances with $W = M^{-2}$.

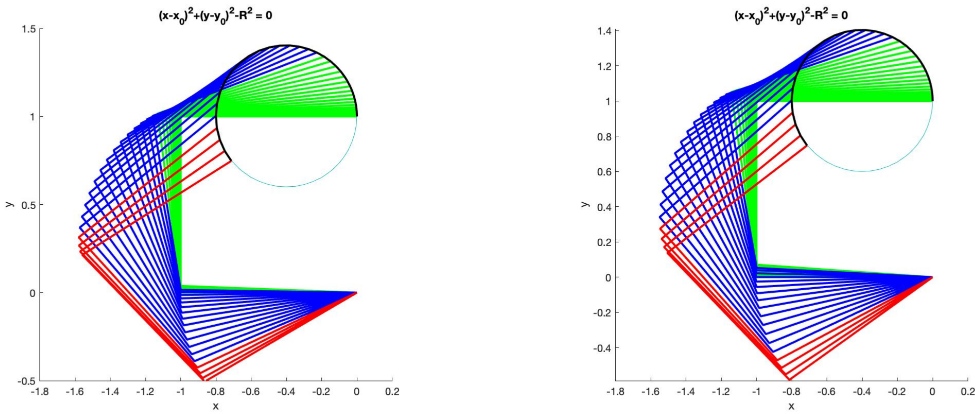

(a) Case $C_1 : \tau_0 = 0$ (b) Case $C_2 : \tau_0 \neq 0$

Figure 26: Partial stroboscopic view , T_{long}

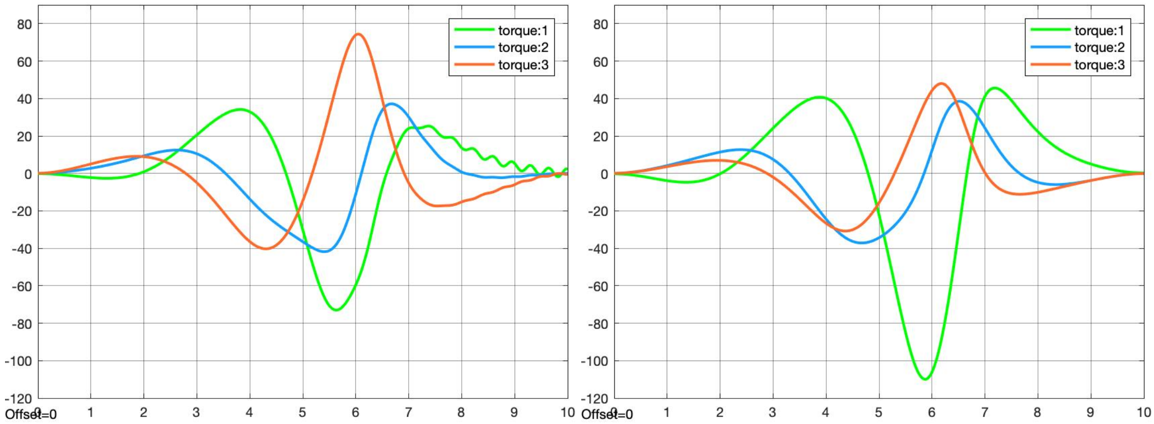

(a) Case $C_1 : \tau_0 = 0$ (b) Case $C_2 : \tau_0 \neq 0$

Figure 27: Motor torques , T_{short}

It can be seen how to avoid those oscillations, the toque exerted by motor 1 is more accentuated in the central region.

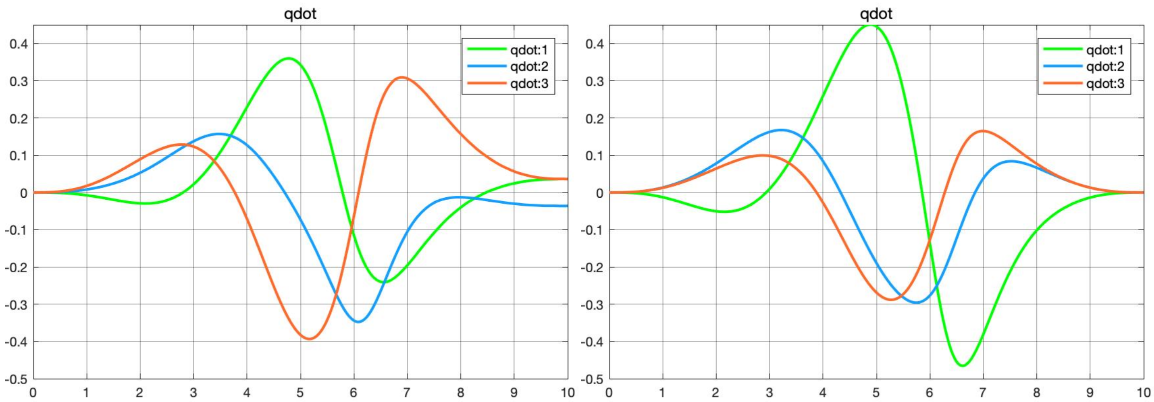

(a) Case $C_1 : \tau_0 = 0$ (b) Case $C_2 : \tau_0 \neq 0$

Figure 28: Joint velocities , T_{short}

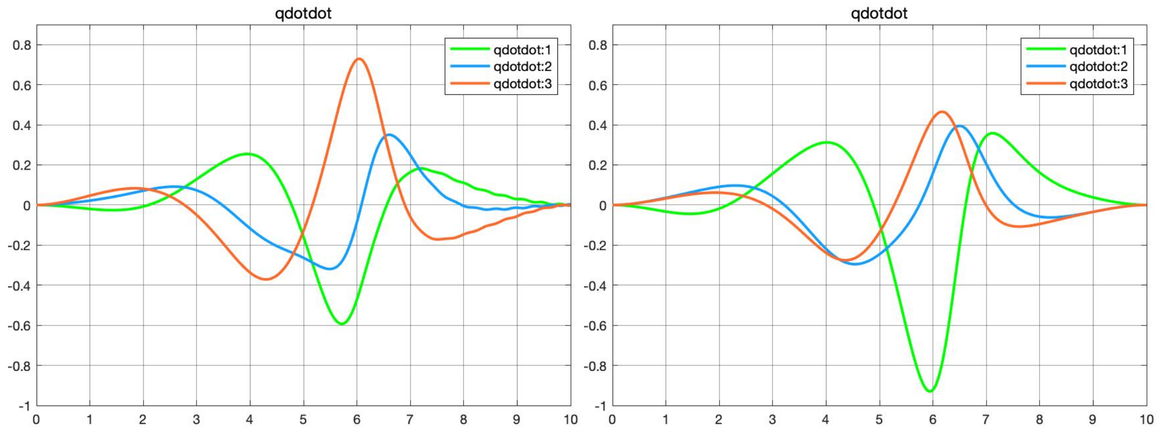

(a) Case $C_1 : \tau_0 = 0$ (b) Case $C_2 : \tau_0 \neq 0$

Figure 29: Joint accelerations , T_{short}

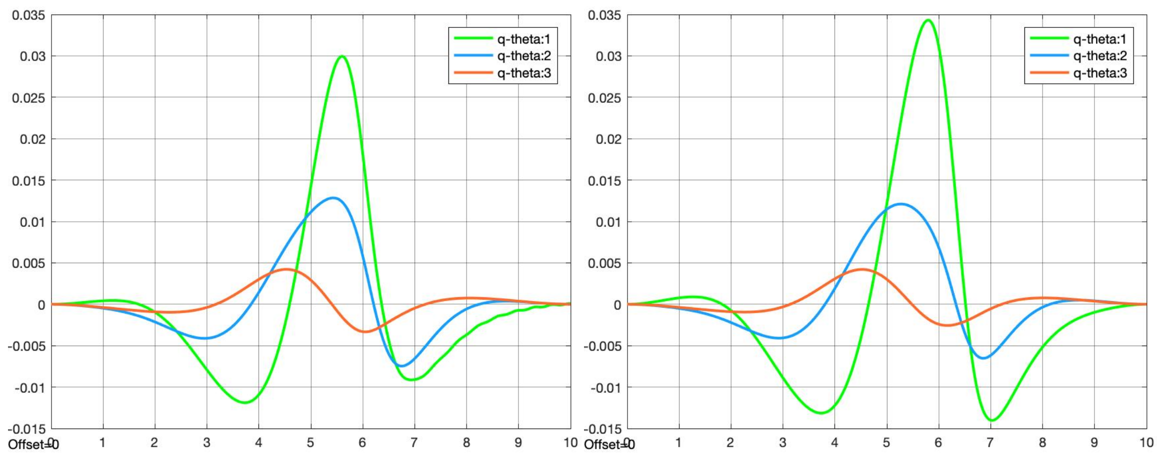

(a) Case $C_1 : \tau_0 = 0$ (b) Case $C_2 : \tau_0 \neq 0$

Figure 30: Error $q - \theta$, T_{short}

The robot movements are even more fluid with M^{-2} w.r.t. M^{-1}, as it is possible to see from the stroboscopic view.

4.3 Rectangular trajectory

It is now shown as a final example a rectangular path. Moreover, an initial error is introduced in order to show the robustness of this method w.r.t initial position error.

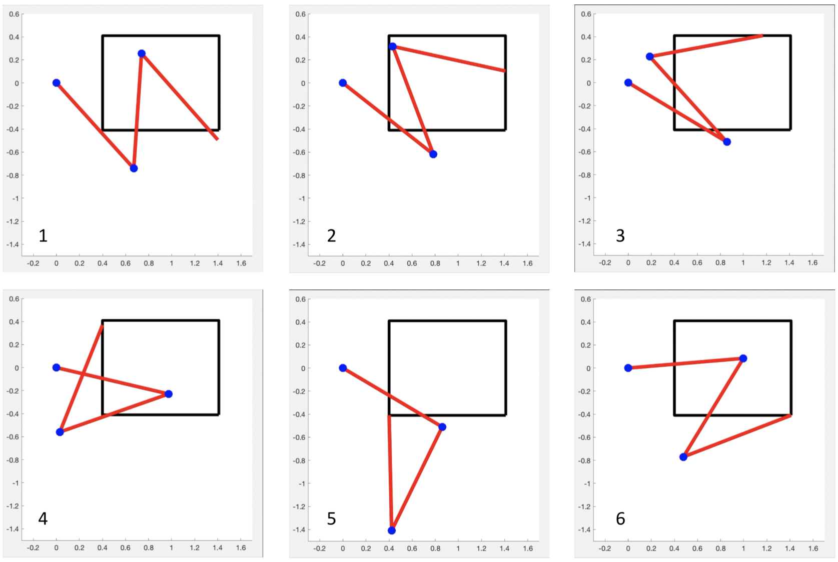

Figure 31: Stroboscopic view of multiline path

A Appendix

A.1 Matrix time derivatives

The simulations presented above contain an algorithm which computes time derivatives for symbolic matrices such as $M(q)$ and $J(q)$, which is based on the following derivation:

$$M(q) \in \mathcal{R}^{n\times m}$$
$$q \in \mathcal{R}^{p}$$

$$\dot{M} = \sum_i \frac{\partial M}{\partial q_i}\dot{q}_i$$

$$\ddot{M} = \sum_i \sum_j \frac{\partial^2 M}{\partial q_i \partial q_j}\dot{q}_i\dot{q}_j + \sum_i \frac{\partial M}{\partial q_i}\ddot{q}_i$$

$$M^{(3)} = \sum_i \sum_j \sum_r \frac{\partial^3 M}{\partial q_i \partial q_j \partial q_r} + \sum_i \sum_j \frac{\partial^2 M}{\partial q_i \partial q_j}\dot{q}_i\ddot{q}_j + 2\sum_i \sum_j \frac{\partial^2 M}{\partial q_i \partial q_j}\ddot{q}_i\dot{q}_j + \sum_i \frac{\partial M}{\partial q_i} q_i^{(3)}$$

where $i, j, r = 1, 2...p$.
In addition, the first and second derivatives of the Coriolis and centrifugal vector$c(q,\dot{q})$

are presented:

$$\dot{c} = \frac{\partial c}{\partial q_i}\dot{q}_i + \frac{\partial c}{\partial \dot{q}_i}\ddot{q}_i$$

A more compact notation can be used in order to compute then the second derivative:

$$X = \begin{pmatrix} q \\ \dot{q} \end{pmatrix}$$

$$\dot{c} = \begin{pmatrix} \frac{\partial c}{\partial q_i} & \frac{\partial c}{\partial \dot{q}_i} \end{pmatrix} \dot{X}$$

$$\ddot{c} = \sum_i \sum_j \frac{\partial^2 c}{\partial x_i \partial x_j} + \sum_i \frac{\partial c}{\partial \dot{x}_i}\ddot{x}$$